Exposed Core Microstructured Optical Fiber Surface Plasmon Resonance Biosensor

Elizaveta Klantsataya[a], Alexandre François[a], Agnieszka Zuber[a], Valeria Torok[ab], Roman Kostecki[a] and Tanya M. Monro[a]

[a]Institute for Photonics and Advanced Sensing (IPAS) and School of Chemistry and Physics, The University of Adelaide, Adelaide, Australia;
[b]South Australian Research and Development Institute (SARDI), Adelaide, Australia

ABSTRACT

Surface Plasmon Resonance (SPR) scattering offers significant advantages compared to traditional reflectivity measurements, essentially turning a non-radiative process into a radiative one. Recently, we have shown that SPR scattering can be used in an optical fiber, enabling higher signal to noise ratio, reduced dependence on the metallic thickness as well as the unique capability of multiplexed detection with a single fiber. Here we report a novel SPR scattering based sensor fabricated based on an exposed-core silica Microstructured Optical Fiber (MOF). This MOF presents a structure with a relatively small core ($\emptyset = 10\mu m$), exposed along the whole fiber length. This exposed core MOF allows for fabrication of SPR supporting metallic thin films directly onto the fiber core offering the new prospect of exploiting SPR in a waveguide structure that supports only a relatively small number of guided optical modes, with a structure that offers ease of fabrication and handling. A thin silver film of 50 nm thickness was deposited onto the fiber core by thermal evaporation. The significant surface roughness of the prepared metallic coatings facilitates strong scattering of the light wave coupled into the surface plasmon. Performance characteristics of the new exposed core fiber sensor were compared to those of a large bare core silica fiber ($\emptyset = 140\mu m$). Although sensitivity of both sensors was comparable (around $2500nm/RIU$), full width at half maximum (FWHM) of the SPR peaks for the new exposed core fiber sensor decreased by a factor of 3 offering an significant enhancement in the detection limit of the new sensing platform in addition to the prospect of a sensor with a lower detection volume.

Keywords: Surface Plasmon Resonance, Optical Fibre, Biosensor

1. INTRODUCTION

Over the past decade, Surface Plasmon Resonance (SPR) sensors have been widely used to detect small changes in the refractive index of an adjacent dielectric. The major application area for SPR sensors is detection of binding of biological molecules which induces changes in the refractive index in the close vicinity of the sensor surface. Several commercial SPR systems, including well-known Biacore*, have been developed.[1] The majority of SPR sensing system, including all commercially available SPR sensors, are based on a high refractive index prism coated with a thin metallic film, often gold, to provide long term stability.[1,2] Some research groups have made significant progress in using optical fibres instead of prism for SPR applications.[3–6] Usage of optical fibres coated with thin metal film allows for creation of miniature SPR sensors that offer advantages of low cost, portability, accessibility, increased dynamic range, etc.

Recently, we reported a novel SPR interrogation method that takes advantages of light scattered by the plasmonic wave facilitated by rough metal coating. Instead of analysing light transmitted through an optical fibre and inferring the existence of a surface plasmon from absorption, this new SPR mechanism allows for collection of scattered light directly above the sensor surface.[7,8] This method allows to create more compact and robust sensing architectures as well as to realise multiple sensing regions for dynamic self referencing and multiplexed sensing. Moreover, it is possible to combine SPR technique with fluorescent sensing.[9]

Most of the recent works have been centered around improvement of performance characteristics of SPR devices. One of the important performance characteristics is sensitivity which is defined as a change of the monitored parameter (such as

Send correspondence to Elizaveta Klantsataya: elizaveta.klantsataya@adelaide.edu.au, telephone: +61 8 8313 0589
*Biacore is a life science products company that uses SPR technology and is owned by GE Healthcare (www.biacore.com)

wavelength or angle of incidence) with respect to a change in the parameter to be determined (refractive index).[10] Increase in a refractive index of a prism or a waveguide shifts the resonant condition towards a longer wavelength and gives rise to the sensitivity of the sensor.[11] A choice of metal also affects sensitivity of SPR sensors. For example, silver offers higher sensitivity in comparison with gold films. Other metals, alloys and multilayer systems have also been used to increase sensitivity of SPR sensors.[12–14] Other factors, such as thickness of the metallic layer and type of excitation used, may influence sensitivity but to a smaller extent.[11]

Increasing sensitivity through lowering the refractive index of a waveguide is a straight forward approach but it results in increase of the line width of SPR curves that in turn increases the resolution and detection limit of the SPR system. Line width primarily depends on geometry of an SPR system and materials that constitute the sensor. Choice of a dielectric material of a waveguide is often a trade off between sensitivity and line width, therefore, geometry of an SPR device is usually modified to improve line width without significantly affecting sensitivity. In particular, reducing size of the fibre core allows to achieve desired improvement in the full width at half maximum (FWHM) for SPR responce. Various alternative geometries have been proposed including tapered fibre designs,[15–17] U-shaped fibres,[18] as well as using single mode fibres (SMF)[19,20] for SPR sensor fabrication. The main challenge for those small core fibres is their fragility which makes it impossible to implement in any real-world application.

Here, we propose a novel SPR fibre sensor that is based on silica exposed core microstructured optical fibre (MOF) developed by Kostetski et al.[21] Supporting microstructure provides a means for protecting a micrometer scale fragile fibre core. The core is exposed along the whole fibre length allowing for deposition of SPR supporting metallic thin film directly on the core. This design offers an advantage of SPR in a waveguide that supports only a limited number of guided modes reducing line width of the SPR curves and, at the same time, provides ease of fabrication and handling. The silica exposed core MOF design is similar to the one developed earlier by Warren-Smith et al. for F2 glass material.[22] Here, using fused silica instead of higher refractive index glass provides mechanical strength as well as higher sensitivity for SPR sensors. In addition to that, the platform exploits the scattering interrogation mechanism that features lower dependency on the quality and thickness of the metallic film, higher signal to noise ratio, and others. In this paper, we present theoretical modelling for large and an attempt to model SPR in small core fibres, and compare it with experimental data obtained for small and large core SPR sensors to estimate improvement in performance of our new SPR device.

2. MATERIALS AND METHODS

2.1 SPR sensor fabrication

Two types of SPR sensors have been fabricated. The first sensor type was constructed from an unstructured (bare core) optical fibre made of fused silica glass (F300) with refractive index of 1.458 and core diameter of $140\mu m$. The fibre was produced in-house by drawing a fused silica rod purchased from Heraeus Quarzglas GmbH & Co. into a fibre using a soft glass drawing tower. The fibre was coated with a polymer cladding with refractive index of 1.325 yielding the numerical aperture of 0.61. A short section of the fibre ($\approx 10mm$) was stripped off the polymer cladding to expose the silica core and the exposed region was coated with thin silver film of $\approx 50nm$ in thickness by using chemical electroless plating. The exposed fibre regions were sonicated in a surface active cleaning agent (Decon90) for 15 min and subsequently rinsed in the ultrasonic bath for 15 min prior silver deposition.

Chemical electroless plating, also known as silver mirror reaction or Tollens reaction, is based on the reduction of silver ammonium complexes in a presence of a reducing agent, such as glucose, into silver nanoparticles that can later be attached to a substrate (glass fibre). The preparation of the reagents starts with the precipitation of an aqueous silver nitrate solution ($20mL$ of $0.24mol/L$ $AgNO_3$), into silver oxide nanoparticles using potassium hydroxide ($40\,\mu\,L$ of $0.25mol/L$ KOH) according to the equation 1. This produces a brown precipitate of silver oxide in the initially transparent solution.[23]

$$2AgNO_3 + 2KOH \rightarrow Ag_2O(s) + 2KNO_3 + H_2O \tag{1}$$

Ammonia ($3mol/L$) is then added drop by drop in order to dissolve the silver oxide and produce a transparent silver ammonium complex ($Ag(NH_3)2NO_3$) (equation 2).

$$Ag_2O(s) + 4NH_3 + 2KNO_3 + H_2O(l) \rightarrow 2Ag(NH_3)_2NO_3 + 2KOH \tag{2}$$

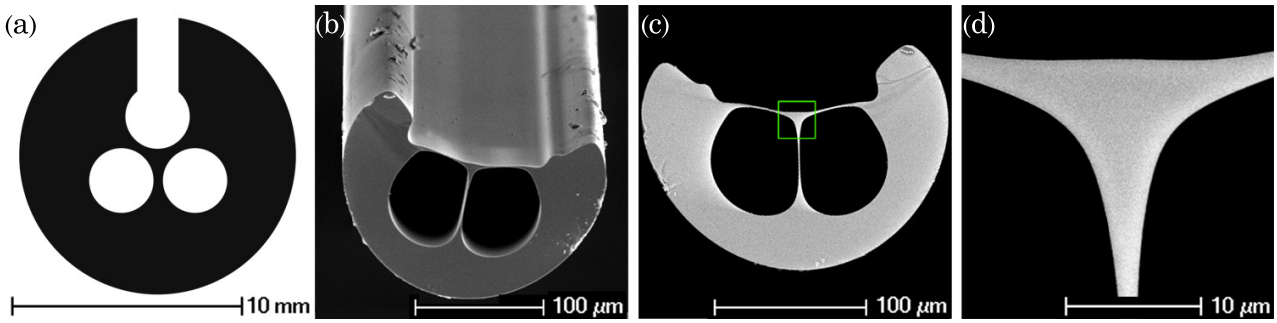

Figure 1. (a) Cross section of the exposed core MOF preform; and, scanning electron microscope images of (b) the silica exposed-core fibre with (c) the cross section measured at the maximum to be $\emptyset 202\mu m$; and, (d) an enlarged image of the core having an effective diameter of $10.0\mu m$.[21]

The reducing agent is a $1:2$ mixture of methanol and glucose ($1.9mol/L$) solution. Once the reducing agent is added to the silver ammonia solution, a metallic silver coating is produced (equation 3).

$$CH_2OH(CHOH)_4CHO + 2Ag(NH_3)_2 + 3OH^- \rightarrow 2Ag(s) + CH_2OH(CHOH)_4CO_2^- + 4NH_3 + 2H_2O \quad (3)$$

The method of chemical deposition of silver was chosen for large bare core fibres as it allows to deposit thin silver films of required thickness of $50nm$ on the whole circumference of the cylindrical fibre core. Moreover, coating produced by this technique features high surface roughness ($7.92 \pm 0.55nm$ measured by Atomic Force Microscopy) that is suitable for scattering interrogation used to analyse SPR.

The second type of SPR sensors was fabricated using exposed core MOF. The exposed-core fibre preform was fabricated from F300HQ silica rod, which was drilled with three holes. The centres of the holes form an equilateral triangle. A slot was cut along the whole length of one of the holes.[21,24] The preform and drawn fibre images are shown on Figure 1. The fibre was cleaned by soaking a middle section of the fibre in a detergent (Decon90) for 30 min with subsequent rinsing in de-ionized water for 30 min and thoroughly dried in air. A short section of the cleaned exposed core fibre ($\approx 10mm$ in length) was coated with silver using thermal vacuum evaporation technique.

Thermal evaporation was performed under vacuum at $2 \times 10^{-4}Pa$ using JEOL thermal evaporator JEE 420. Evaporation source of fine silver granules purchased from Peter W Beck Pty. Ltd. was evaporated using tungsten wire crucible at $28Amps$. Due to the difficulty of the characterisation of small cylindrically shaped fibres, the characterisation of produced thin films was performed indirectly by analysing glass slides coated together with the fibres. The thickness of the produced coatings was determined by measuring the transmission at $632nm$ with an absorption coefficient assumed to be $\alpha = 9.9134 \times 10^5 cm^{-1}$ and was measured to be $46.5 \pm 1.5nm$. Surface roughness of $4.13 \pm 0.38nm$ was measured by Atomic Force Microscopy (NT-MDT Ntegra Solaris AFM).

2.2 Optical setup

To analyse the SPR response, we used an in-house built SPR setup as depicted on the Figure 2. A broad band light source (Supercontinum White Light Laser KOHERAS SuperK Compact) was launched into a fibre with a sensing region located in the middle of the fibre length. The sensing region was immersed into a flow cell with an inlet and an outlet for flowing liquid samples through the sensor. The flow cell had a transparent window allowing for collection of scattered light above the sensing region. The scattered light collection apparatus consisted of an objective, a converging lens, and an optical fibre bundle to transfer the collected light to the Ocean Optics compact spectrometer (QE 65000) for characterisation. Light transmitted through the optical fibre was projected onto a screen to ensure coupling into a core as opposed to supporting structure in the case of exposed core MOF based sensors.

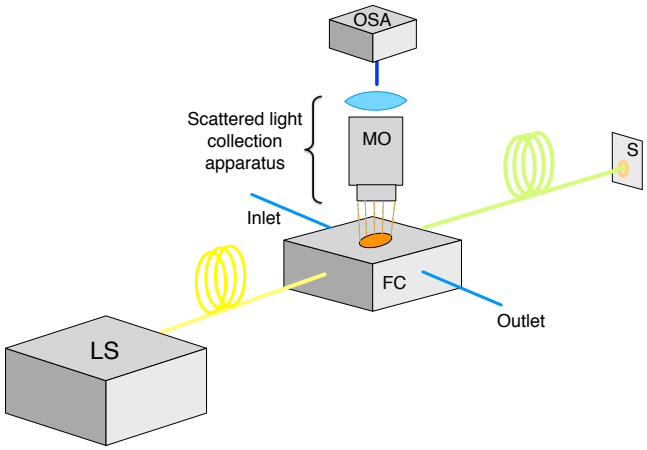

Figure 2. Optical setup. LS - broadband light source, FC - flow cel with sensing region of the fibre in the centre, MO - microscope objective, S - screen, OSA - optical spectral analyser.

2.3 Definition of sensor performance characteristics

Sensitivity of an SPR sensor is defined as a change of the monitored parameter (such as wavelength or angle of incidence) with respect to a change in the parameter to be determined (refractive index). For wavelength interrogation based sensors sensitivity could be written as:

$$S_\lambda = \frac{\delta\lambda}{\delta n} \tag{4}$$

The refractive index sensitivity S_λ for the SPR sensors was determined by measuring a wavelength shift $\delta\lambda$ for a known change in a refractive index (RI) of a sample δn (serial dilutions of glycerol in de-ionized water).

Resolution of an SPR sensor is defined as the minimum change in the refractive index that could be resolved by the sensor. Resolution depends on the system noise which in turn is influenced by ambient temperature, photodetector noise, and the light source. Sensor resolution increases as the line width of SPR signal decreases.[14] Resolution can be calculated as an average of noise contribution from three sources:

$$R = 3\sigma = 3\sqrt{\sigma_{ampl}^2 + \sigma_{spectral}^2 + \sigma_{thermal}^2} \tag{5}$$

where σ_{ampl} is noise contribution from the signal amplitude, $\sigma_{spectral}$ - noise contribution from spectral position, and $\sigma_{thermal}$ - thermal noise. Noise contribution from the signal amplitude depends on full width at half maximum (FWHM) of the SPR signal and is defined[25] as:

$$\sigma_{ampl} = \frac{FWHM}{4.5(SNR)^{0.25}} \tag{6}$$

Detection Limit is another important performance characteristic of SPR sensing devices. For a given sensitivity S and resolution R of a sensor, detection limit DL is defined as ratio:

$$DL = \frac{R}{S} \tag{7}$$

For refractive index sensors, detection limit defines the smallest change in a refractive index of a sample (sensor resolution) that could be measured accurately (with given sensitivity) by the sensor. For biomolecular sensing, the detection limit is often defined as the minimum amount of analyte that could be quantified by the biosensor.

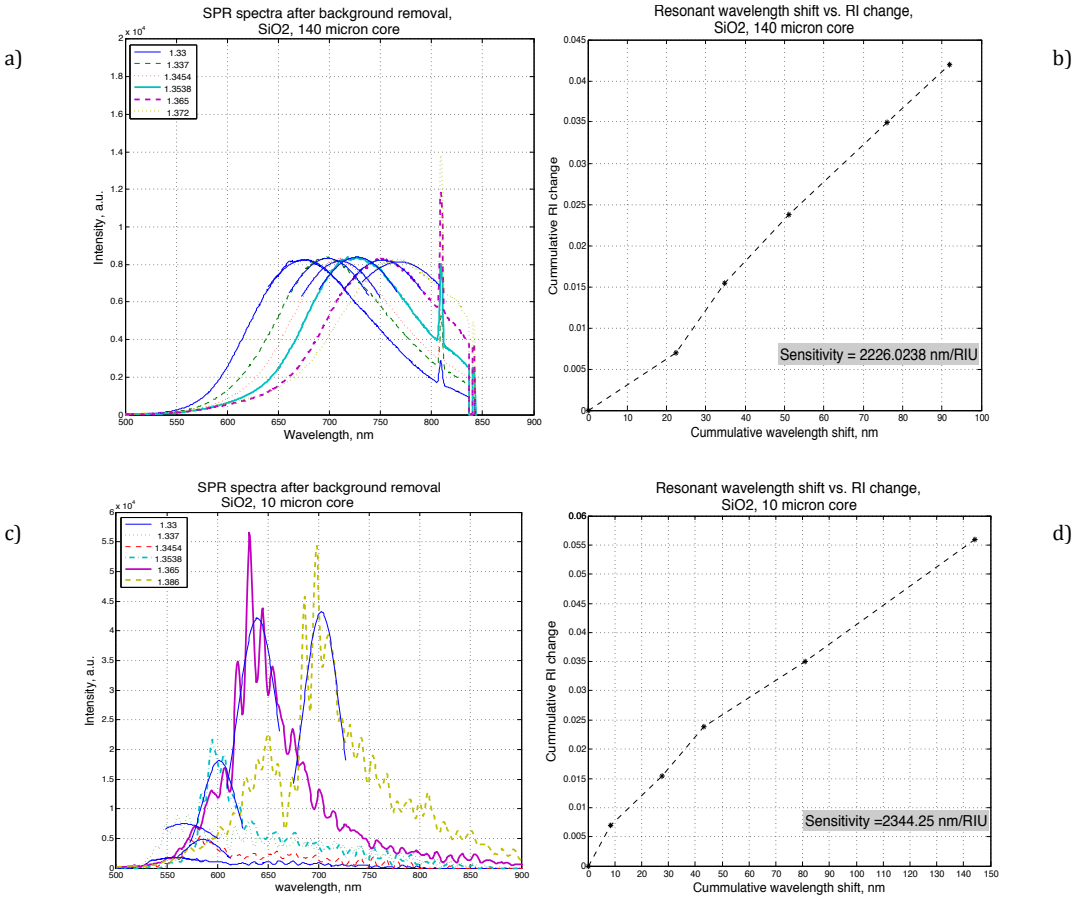

Figure 3. a) Collected SPR spectra for $140\mu m$ bare core silica fibre sensor. Sensors prepared by chemical electroless plating of silver films of $50nm$ thickness. Solid curves show Gaussian fit of the experimental data near the peak. Legend show different refractive indices of the sensing medium. b) Cumulative resonant wavelength shift vs. cumulative change in a refractive index of the sensing medium. Slope of the curve gives value of the sensitivity.
c) Collected SPR spectra for $10\mu m$ exposed core MOF sensor. Sensors prepared by thermal vacuum evaporation of silver films of $50nm$ thickness. Solid curves show Gaussian fit of the experimental data near the peak. Legend show different refractive indices of the sensing medium. d) Cumulative resonant wavelength shift vs. cumulative change in a refractive index of the sensing medium. Slope of the curve gives value of the sensitivity.

2.4 Experimental results for sensitivity and line width

Bare core fibres of $140\mu m$ core diameter and exposed core fibres with $10\mu m$ core diameter with sensing regions have been prepared. In order to estimate performance characteristics of the sensors, the sensing regions of the fibres were immersed in the liquids with different known refractive indices ranging from 1.33 to 1.386 (serial dilutions of glycerol in de-ionized water). The broadband light was coupled into one end of a sensing fibre and scattered light was collected using fibre bundle with microscope objective placed in a close vicinity of the sensing region as described in the section 2. In the case of bare core fibres, sensing regions were placed in a flow cell to facilitate data collection. The flow cell had an inlet and an outlet for flowing liquids through the cell and a glass window on the top for scattered light collection. Measurements before immersion in glycerol served as reference spectra. The collected evanescent field measurements are shown on left plots on Figure 3. High noise in the experimental measurements for the exposed core fibres are caused by the fact that the flow cell was not used and therefore, was not blocking out the background light leaking from the supporting fibre structure.

The raw spectrum data has been fitted to a Gaussian function expressed by the equation 8. Peaks of the fitted functions have been found and positions of the peaks in a spectral domain (resonant wavelength) have been recorded. In order to find sensitivity for a sensor, a plot of cumulative refractive index changes versus cumulative resonant wavelength shifts were

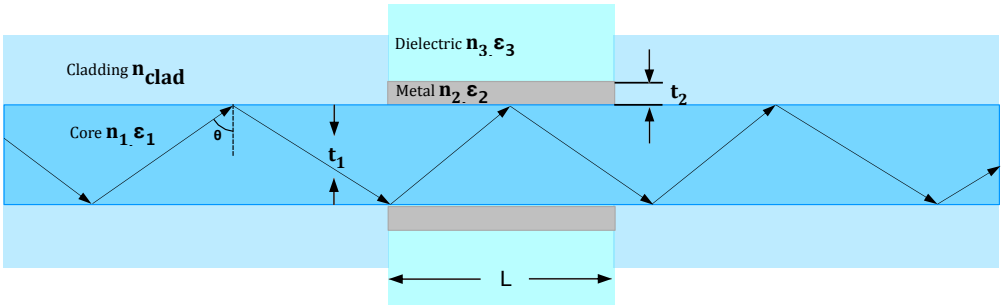

Figure 4. Model for the large core SPR fibre sensor.

built. Those plots are presented on Figure 3 (a) and (b) for bare core fibre sensors and for the exposed core fibre sensors respectively. Value of sensitivity is found as a slop of those curves. FWHM is found as spectral width of the individual SPR spectrum curves at half maximum and is averaged for a particular sensor.

$$y = Ae^{\frac{-(x-\mu)^2}{2\sigma^2}} \tag{8}$$

Table 1 summarises experimental results for large bare core and exposed core sensors.

Table 1. Experimental results for sensitivity and FWHM for two types of SPR sensors.

Type of SPR sensor	Bare core, $140\mu m$	Exposed core, $10\mu m$
Sensitivity, nm/RIU	2226.02 ± 571	2344.25 ± 777
FWHM, nm	141.4 ± 10.84	44 ± 3.94

3. RESULTS AND DISCUSSION

Sensitivity as well as line width as one of the measures of detection limit for SPR sensors have been estimated using theoretical modelling. The purpose of the modelling is to investigate how the size of the fibre core from which SPR is exited influence performance characteristics of the sensors, in particular, sensitivity and FWHM of SPR response curves. As it was observed experimentally that line width of SPR response decreases as the core size decreases, modelling of SPR for fibres with different core diameter has been done. Two models described in subsections 3.1 and 3.2 were used to study large core and small core fibre SPR sensors.

3.1 Theoretical modelling for large core fibres

Large core multimode fibres could be approximated by the laws of geometrical optics. SPR in large core multimode fibres could be successfully modelled using Fresnel reflection equations.[12,26,27] Three layers have been considered in the modelling: silica fibre core, silver film, and a dielectric sample. A schematic on Figure 4 illustrates the model and related parameters.

We assume that the dielectric function of silver is defined by the Drude's model:[26]

$$\epsilon_m(\lambda) = 1 - \frac{\lambda^2 \lambda_c}{\lambda_p^2(\lambda_c + i\lambda)}, \tag{9}$$

where $\lambda_c = 1.7614 \times 10^{-5}$ is a collision wavelength of silver, $\lambda_p = 1.4541 \times 10^{-7}$ - plasma wavelength of silver.[26]

A multilayer matrix method was used to calculate reflection coefficients for p-polarised light:[26,27]

$$R_p = |r_p|^2, \tag{10}$$

where amplitude reflection coefficient r_p is defined by:

$$r_p = \frac{(M_{11} + M_{12}q_N)q_1 - (M_{21} + M_{22}q_N)}{(M_{11} + M_{12}q_N)q_1 + (M_{21} + M_{22}q_N)}, \tag{11}$$

where M_{mn} are components of characterisation matrix that relates fields at the first boundary to the fields at the last boundary:

$$M = \prod_{k=2}^{N-1} M_k = \begin{bmatrix} M_{11} & M_{12} \\ M_{21} & M_{22} \end{bmatrix}, \tag{12}$$

with

$$M_k = \begin{bmatrix} cos\beta_k & (-isin\beta_k)/q_k \\ -iq_k sin\beta_k & coas\beta_k \end{bmatrix}, \tag{13}$$

where $q_k = \sqrt{\frac{\mu_k}{\epsilon_k}} cos\theta_k = \frac{\sqrt{\epsilon_k - n_1^2 sin^2\theta_1}}{\epsilon_k}$, and $\beta_k = \frac{2\pi}{\lambda} n_k cos\theta_k t_k = \frac{2\pi t_k}{\lambda}\sqrt{\epsilon_k - n_1^2 sin^2\theta_1}$. The layers $1...N$ of thickness t_k, dielectric constant ϵ_k, permeability μ_k and refractive index n_k are assumed to be stacked together.

Assuming a collimated light source, angular power distribution of the guided rays in a fibre is proportional to:

$$dP \propto \frac{n_1^2 sin\theta cos\theta}{(1 - n_1^2 cos^2\theta)^2} d\theta. \tag{14}$$

A generalised expression for normalised transmitted power in a fibre considers the number of reflections a specific ray travelling at a certain angle undergoes with a sensor surface and could be written as:

$$P = \frac{\int_{\theta_{cr}}^{\pi/2} R_p^{N(\theta)} \frac{n_1^2 sin\theta cos\theta}{(1 - n_1^2 cos^2\theta)^2} d\theta}{\int_{\theta_{cr}}^{\pi/2} \frac{n_1^2 sin\theta cos\theta}{(1 - n_1^2 cos^2\theta)^2} d\theta}, \tag{15}$$

where $N(\theta) = \frac{L}{t_1 tan\theta}$ is a number of reflections a certain ray travelling at an angle θ makes within the sensing region of length L, and $\theta_{cr} = sin^{-1}(n_{clad}/n_1)$ is a critical angle for the fibre.

Fused silica was used as a core material and silver of thickness $50nm$ was used as an SPR supporting material to match experimental settings. Core diameter was varied within range of $100\mu m$ to $300\mu m$. The result of the modelling is presented on the Figure 5. It is worth mentioning that geometrical optics approximation is known to be valid for fibre diameters larger than $100\mu m$.[28] The theoretical result suggests that sensitivity does not have a strong dependency on the core size and is around $5850nm/RIU$. The high value of sensitivity predicted theoretically was observed experimentally but with low reproducibility. It could be explained by the fact that silver coating oxidises rapidly and the presence of oxides changes dielectric function of the metallic film. The wide range of the experimentally measured sensitivity for sensors prepared by chemical electroless plating (Table 2) is also likely to be due to presence of silver oxides in the films. As far as FWHM is concerned, it monotonically increases with increasing core diameter. This result is consistent with experimentally observed tendency described in the subsection 2.4.

Table 2 summarises experimental and theoretical values for sensitivity and FWHM of sensors with different core diameters.

Table 2. Comparison of theoretical and experimental results for small and large core silica fibres with silver film.

Source	**Sensitivity, nm/RIU**	**FWHM, nm**
Theoretical modelling ($140\mu m$ core diameter)	≈ 5800	≈ 150
Experimental data ($140\mu m$ core diameter)	$\approx 2000 - 5500$	≈ 150
Experimental data ($\approx 1 - 10\mu m$ core diameter)	≈ 2500	≈ 50

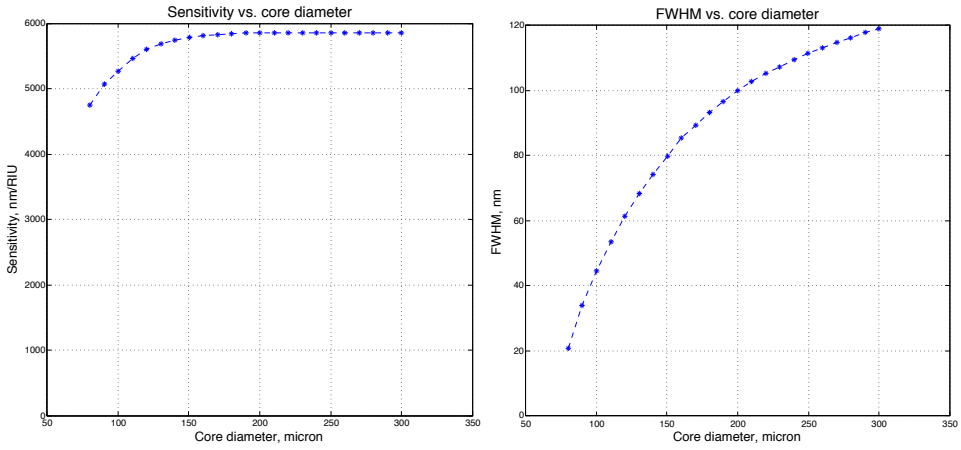

Figure 5. Left: Theoretical dependence of sensitivity of an SPR sensor based on a large core silica fibre. Right: Theoretical dependence of FWHM of SPR response for a large core silica SPR sensor. SPR supporting metal is assumed to be silver film of thickness $50nm$. Refractive indices of the seeing dielectric medium is varied in range of $[1.33, 1.35]$.

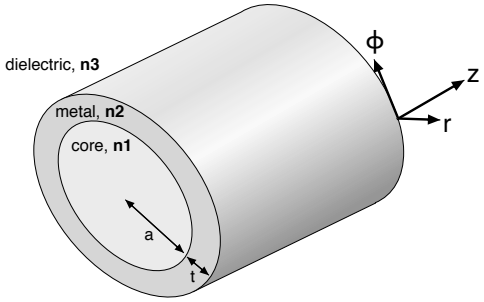

Figure 6. Model for the small core SPR fibre sensor.

3.2 Theoretical modelling for small core fibres

The experimental data obtained for small core SPR sensors shown that FWHM of SPR signal is significantly smaller that that for large core SPR sensors. In order to investigate this theoretically, we attempted to model SPR in small core fibres. In order to be able to model SPR in fibres where a core diameter is an order of few micron, electromagnetic nature of light need to be taken into account. We consider a 3-layer structure of cylindrical dielectric core, coated with coaxial metallic sheath and the whole structure is surrounded by another dielectric of sufficient enough thickness that mode fields decay completely within it. The schematic of the model is illustrated on the Figure 6.

We make an assumption that all field components vary as $e^{(in\phi+i\beta z-i\omega t)}$, where n is azimuthal mode order number, and $\beta = k_0 n_e$ is a propagation function, with n_e - effective mode index and k_0 - the wave number of free space.[29] Solving Maxwell's equations for each of the three layers, we find expressions for the tangental field components E_z, H_z, E_ϕ, and H_ϕ for the core, metal, and outer dielectric layers. Than, matching the tangental filed components at the boundaries of core-metal ($r = a$) and metal-dielectric ($r = a + t$), we find the dispersion relation.[29] All functions are evaluated in the complex domain and modified Bessel functions are used since the dielectric function of metal is considered in its complex form. The existence of Surface Plasmon is inferred from detecting a peak in the imaginary part of the effective index of the fibre mode that correspond to the maximum attenuation due to the coupling of the fibre mode to the surface mode.

Essentially, any parameter of the model (core size a, core material, metal, metal film thickness t, azimuthal mode order number n, outer dielectric index n_3) could be varied. For the purposes of modelling SPR in a structure similar to that used experimentally, as well as studying influence of the core size on SPR performance characteristics, the following parameters of the model were fixed –

- Core material, n_1 - fused silica which refractive index was modelled using Sellmeier relation:[28]

$$n_1(\lambda) = \sqrt{1 + \frac{B_1\lambda^2}{\lambda^2 - C_1^2} + \frac{B_2\lambda^2}{\lambda^2 - C_2^2} + \frac{B_3\lambda^2}{\lambda^2 - C_3^2}}, \tag{16}$$

  where B_1 = 0.68374049400, B_2 = 0.42032361300, B_3 = 0.58502748000, C_1 = 0.00460352869, C_2 = 0.01339688560, C_3 = 64.49327320000;

- Metal, n_2 - silver was modelled using Drude-Lorentz model for the dielectric constant of metals;[30]
- Silver film thickness t of $50nm$;
- Radial mode oder number $p = 1$, as higher radial order modes do not evolve into surface modes due to their oscillatory behaviour within the fibre core.[29]

The following parameters of the model were varied –

- Core diameter $2a \in [0.2, 10]\mu m$;
- Outer dielectric refractive index $n_3 \in [1.33, 1.34]$;
- Azimuthal mode order number $n \in [1, 10]$.

It has been found that for small core fibres the theoretical value of the FWHM increases with increasing core size and is around $20 - 60nm$ for the core diameters considered in the calculations ($1 - 10\mu m$). However, fibres with core diameter of $10\mu m$ that have been used experimentally have a large number of guided modes. At this stage, we consider the contribution of every mode separately. In reality, the overall SPR response would be a convolution of all the guided modes that evolve into surface plasma modes. Making this assumptions significantly simplifies the analysis and as a preliminary theoretical modelling is sufficient for giving a trend of the FWHM. In order to be able to assess contribution of all the guided modes to the SPR, power distribution of the modes needs to be considered. This is an ongoing work that we plan to accomplish.

CONCLUSION

We developed a new type of SPR fibre sensor based on exposed core MOF that features small core with easy handling of the fragile optical fibre. Usage of the small core provides advantages of decreased line width of SPR signal and therefore lowers the detection limit without sacrifice in sensitivity of the sensor. The utilisation of the smaller core fibre is combined with earlier developed novel interrogation method where light scattered by surface plasmon is collected and analysed. This in turn provides improved signal to noised ratio, lower dependency on the metal film thickness as well as other practical advantages.

In this work, we theoretically investigated the effect of changing fibre core size on SPR sensor performance characteristics, in particular, sensitivity and line width of SPR response. We have found that sensitivity is not significantly affected by core size and is more a property of materials constituting the sensor such as metal and core glass. As far as line width is concerned, using smaller core fibre results in narrower SPR peaks which provides lower resolution and detection limit. It has been estimated that the improvement in the line width of SPR response for exposed core fibre based SPR sensor is a factor of 3 in comparison with using large bare core fibres. Although the experimentally observed result for exposed core fibres is consistent with theoretically predicted values for FWHM, there is a significant scope for further work on theoretical modelling of SPR in small waveguides that would take into account power distribution of the guided modes.

In addition, we experimentally demonstrated the fabrication of the exposed core based SPR fibre sensor and compared its performance characteristics with large bare core SPR sensors. The experimental improvement of the line width of SPR signal for exposed core sensors is consistent with theoretically predicted values and is estimated to be a factor of 3 in comparison with large core SPR sensors. Even though, the results are preliminary, we were able to demonstrate that utilisation of the new exposed core SPR sensor is a powerful approach to reduce SPR line width and thus decrease the detection limit of an SPR device which opens opportunities for development of SPR platforms for new biosensing applications.

ACKNOWLEDGMENTS

T. Monro acknowledges the support of an ARC Federation Fellowship as well as the support of DSTO Australia for this work. This work was performed at the Optofab node of the Australian National Fabrication Facility, a company established under the National Collaborative Research Infrastructure Strategy to provide nano and microfabrication facilities for Australia's researchers. The authors also want to acknowledge S. Warren-Smith, H. Ebendorff-Heidepriem, and P. Henry for contribution to fibre fabrication, and S. Afshar Vahid for contribution to theoretical modelling.

REFERENCES

[1] Homola, J., Yee, S. S., and Gauglitz, G., "Surface plasmon resonance sensors: review," *Sensors and Actuators B: Chemical* **54**(1 - 2), 3 – 15 (1999).

[2] Homola, J., "Present and future of surface plasmon resonance biosensors," *Analytical and Bioanalytical Chemistry* **377**, 528–539 (2003).

[3] Albert, J., Shao, L.-Y., and Caucheteur, C., "Tilted fiber bragg grating sensors," *Laser & Photonics Reviews* **7**(1), 83–108 (2013).

[4] Slavık, R., Homola, J., Čtiroki, J., and Brynda, E., "Novel spectral fiber optic sensor based on surface plasmon resonance," *Sensors and Actuators B: Chemical* **74**, 106 – 111 (2001). Proceedings of the 5th European Conference on Optical Chemical Sensors and Biosensors.

[5] Kim, S. A., Kim, S. J., Moon, H., and Jun, S. B., "In vivo optical neural recording using fiber-based surface plasmon resonance," *Opt. Lett.* **37**, 614–616 (Feb 2012).

[6] Lin, Y.-C., "Characteristics of optical fiber refractive index sensor based on surface plasmon resonance," *Microwave and Optical Technology Letters* **55**(3), 574–576 (2013).

[7] Sciacca, B., François, A., Hoffmann, P., and Monro, T. M., "Multiplexing of radiative-surface plasmon resonance for the detection of gastric cancer biomarkers in a single optical fiber," *Sensors and Actuators B: Chemical* **183**(0), 454 – 458 (2013).

[8] Sciacca, B., François, A., Klingler-Hoffmann, M., Brazzatti, J., Penno, M., Hoffmann, P., and Monro, T., "Radiative-surface plasmon resonance for the detection of apolipoprotein e in medical diagnostics applications," *Nanomedicine: Nanotechnology, Biology and Medicine* (2012).

[9] François, A., Boehm, J., Oh, S., Kok, T., and Monro, T., "Collection mode surface plasmon fibre sensors: A new biosensing platform," *Biosensors and Bioelectronics* **26**(7), 3154 – 3159 (2011).

[10] Homola, J., [*Surface Plasmon Resonance Based Sensors*], Springer series on chemical sensors and biosensors, Springer (2006).

[11] Homola, J., "On the sensitivity of surface plasmon resonance sensors with spectral interrogation," *Sensors and Actuators B: Chemical* **41**(1-3), 207 – 211 (1997).

[12] Sharma, N. K., "Performances of different metals in optical fibre-based surface plasmon resonance sensor," *Pramana - Journal od Physics, Indian Academy of Sciences* **78**, 417–427 (March 2011).

[13] Herminjard, S., Sirigu, L., Herzig, H. P., Studemann, E., Crottini, A., Pellaux, J.-P., Gresch, T., Fischer, M., and Faist, J., "Surface plasmon resonance sensor showing enhanced sensitivity for co2 detection in the mid-infrared range," *Opt. Express* **17**, 293–303 (January 2009).

[14] Lee, K.-S., Son, J. M., Jeong, D.-Y., Lee, T. S., and Kim, W. M., "Resolution enhancement in surface plasmon resonance sensor based on waveguide coupled mode by combining a bimetallic approach," *Sensors* **10**(12), 11390–11399 (2010).

[15] Verma, R., Sharma, A., and Gupta, B., "Modeling of tapered fiber-optic surface plasmon resonance sensor with enhanced sensitivity," *Photonics Technology Letters, IEEE* **19**, 1786 –1788 (nov.15, 2007).

[16] González-Cano, A., Bueno, F.-J., Óscar Esteban, Díaz-Herrera, N., and Navarrete, M.-C., "Multiple surface-plasmon resonance in uniform-waist tapered optical fibers with an asymmetric double-layer deposition," *Appl. Opt.* **44**, 519–526 (Feb 2005).

[17] Kim, Y.-C., Peng, W., Banerji, S., and Booksh, K. S., "Tapered fiber optic surface plasmon resonance sensor for analyses of vapor and liquid phases," *Opt. Lett.* **30**, 2218–2220 (Sep 2005).

[18] Verma, R. K. and Gupta, B. D., "Theoretical modelling of a bi-dimensional u-shaped surface plasmon resonance based fibre optic sensor for sensitivity enhancement," *Journal of Physics D: Applied Physics* **41**(9), 095106 (2008).

[19] Fontana, E., Dulman, H., Doggett, D., and Pantell, R., "Surface plasmon resonance on a single mode optical fiber," *Instrumentation and Measurement, IEEE Transactions on* **47**(1), 168–173 (1998).
[20] Slavık, R., Homola, J., and Čtyrokỳ, J., "Single-mode optical fiber surface plasmon resonance sensor," *Sensors and Actuators B: Chemical* **54**(1), 74–79 (1999).
[21] Kostecki, R., Ebendorff-Heidepriem, H., Davis, C., McAdam, G., Warren-Smith, S. C., and Monro, T. M., "Silica exposed-core microstructured optical fibers," *Opt. Mater. Express* **2**, 1538–1547 (Nov 2012).
[22] Warren-Smith, S. C., Ebendorff-Heidepriem, H., Foo, T. C., Moore, R., Davis, C., and Monro, T. M., "Exposed-core microstructured optical fibers for real-time fluorescence sensing," *Opt. Express* **17**, 18533–18542 (Oct 2009).
[23] Saito, Y., Wang, J., Smith, D., and Batchelder, D., "A simple chemical method for the preparation of silver surfaces for efficient sers," *Langmuir* **18**(8), 2959–2961 (2002).
[24] Kostecki, R., Ebendorff-Heidepriem, H., Warren-Smith, S. C., and Monro, T. M., "Predicting the drawing conditions for microstructured optical fiberfabrication," *Opt. Mater. Express* **4**, 29–40 (Jan 2014).
[25] White, I. M. and Fan, X., "On the performance quantification of resonant refractive index sensors," *Opt. Express* **16**, 1020–1028 (Jan 2008).
[26] Sharma, A. K. and Mohr, G. J., "On the performance of surface plasmon resonance based fibre optic sensor with different bimetallic nanoparticle alloy combinations," *Journal of Physics D: Applied Physics* **41**(5), 055106 (2008).
[27] Chen, Y., Zheng, R., Lu, Y., Wang, P., and Ming, H., "Fiber-optic surface plasmon resonant sensor with low-index anti-oxidation coating," *Chin. Opt. Lett.* **9**, 100605 (Oct 2011).
[28] Saleh, B. and Teich, M., [*Fundamentals of Photonics*], Wiley Series in Pure and Applied Optics, John Wiley & Sons (2007).
[29] Al-Bader, S. J. and Imtaar, M., "Optical fiber hybrid-surface plasmon polaritons," *JOSA B* **10**(1), 83–88 (1993).
[30] Ung, B. and Sheng, Y., "Interference of surface waves in a metallic nanoslit," *Opt. Express* **15**(3), 1182–1190 (2007).